WIDEBAND MICROWAVE GENERATION WITH GAAS PHOTOCONDUCTIVE SWITCHES*

R. L. Druce, M. D. Pocha, K. L. Griffin
Lawrence Livermore National Laboratory
P.O. Box 808, L-153
Livermore, CA 94550

Jeremy M. Stein
Rockwell International
2021 Gerard S.E., Suite 102
Albuquerque, New Mexico 87106

B. James J. O'Bannon
Rockwell International
P.O. Box 3170
Anaheim, California 92803

ABSTRACT

We are using solid state photoconductive switches to generate wideband microwave pulses with peak powers to 20 MW. A parallel-plate Blumlein transmission line is used to directly feed an exponential taper antenna to produce single pulses with rise times of 200 ps and pulse durations of 340 ps (FWHM). Voltages up to 21 kV have been generated in a 1 cm tall, 12 cm wide parallel-plate line. With the switches operated in linear mode, we have demonstrated phasing of several switches to generate a coherent wave. Generated and radiated signals agree very well with numerical calculations. Radiation efficiencies approach 30%. The Blumlein dielectric can be changed to produce a damped waveform, thereby modifying the bandwidth of the signal. We have generated damped waveforms of up to 3 cycles using this method. The parallel-plate geometry lends itself to coupling to an antenna structure to radiate efficiently. The geometry also lends itself to expanding the generator in height and width. We have stacked two generators to nearly double the output power without degrading the pulse characteristics.

Applications of ultrashort microwave pulses (UWB radar, HPM weapons) require a high repetition rate and long life from the generator. Life times of $>10^5$ shots have been seen occasionally at low to medium power densities. As the power density of a solid state photoconductive switch is increased, device life decreases. We have the capability to test devices at a repetition rate of 30 Hz and voltages to 25 kV. Preliminary data indicates that repeated pulse biasing (without switching) of large LEC grown devices in a slab geometry with fields as low as 30 kV/cm damages the switch and eventually leads to failure.

INTRODUCTION

High-power, ultra-wideband (UWB) microwave technology offers significant potential advantages over conventional microwave technology for many applications, including radar, RF weapons, electronic jamming, and secure communications. To take one example the advantages of UWB radar over conventional narrow-band radar would include:

- Improved range resolution
- Target recognition
- Improved penetration of foliage, walls, or ground
- Target discrimination
- Very short range capability (< m)
- Low probability of intercept
- Reduced sensitivity to electronic countermeasures

Until recently, the technology of UWB microwaves was such that many practical applications were not feasible. Now, however, advances in key technologies - ultra-fast solid-state switches, ultra-fast high power lasers, and ultra-wideband antennas - have made possible the development of flexible, efficient UWB high-power-microwave (HPM) generators.

THE MICROWAVE GENERATOR AND ANTENNA

In collaboration with the University of Texas, we developed the microwave generator shown schematically in Fig. 1 and photographically in Fig. 2.

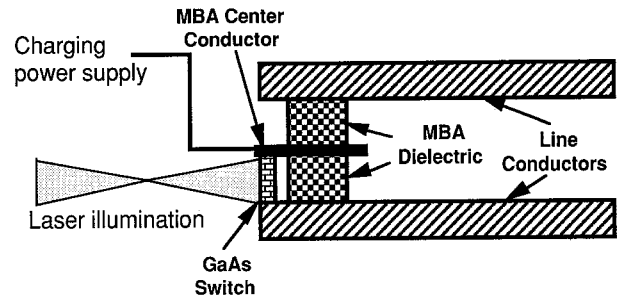

Figure 1. Block diagram of Mismatched Blumlein Aperture microwave generator module.

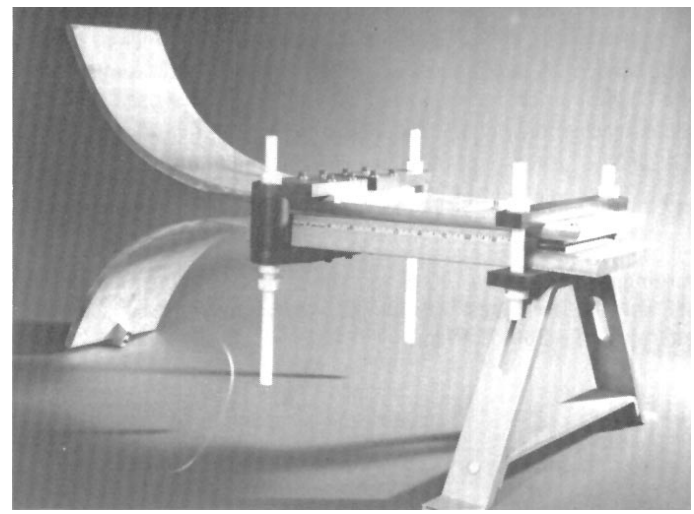

Figure 2. Photograph of MBA module with exponential antenna attached.

The generator is based on a parallel-plate mismatched Blumlein aperture (MBA)[1] feeding a parallel-plate transition/diagnostic section and an exponentially tapered wideband antenna. The mismatched Blumlein aperture approach has several potential advantages over other schemes to generate and radiate UWB signals. In the classic folded Blumlein line, two transmission lines are charged in parallel and discharged in series. If the impedance of the Blumlein is matched to the impedance of the load, a single pulse is delivered to the load equal in

*This work was performed under the auspices of the U.S. Department of Energy by Lawrence Livermore National Laboratory under contract no. W-7405-Eng-48.

Report Documentation Page

Form Approved
OMB No. 0704-0188

1. REPORT DATE	2. REPORT TYPE	3. DATES COVERED
JUN 1991	**N/A**	**-**

4. TITLE AND SUBTITLE	5a. CONTRACT NUMBER
Wideband Microwave Generation With Gaas Photoconductive Switches	5b. GRANT NUMBER
	5c. PROGRAM ELEMENT NUMBER
6. AUTHOR(S)	5d. PROJECT NUMBER
	5e. TASK NUMBER
	5f. WORK UNIT NUMBER
7. PERFORMING ORGANIZATION NAME(S) AND ADDRESS(ES) **Lawrence Livermore National Laboratory P.O. Box 808, L-153 Livermore, CA 94550**	8. PERFORMING ORGANIZATION REPORT NUMBER
9. SPONSORING/MONITORING AGENCY NAME(S) AND ADDRESS(ES)	10. SPONSOR/MONITOR'S ACRONYM(S)
	11. SPONSOR/MONITOR'S REPORT NUMBER(S)

12. DISTRIBUTION/AVAILABILITY STATEMENT
Approved for public release, distribution unlimited

13. SUPPLEMENTARY NOTES
See also ADM002371. 2013 IEEE Pulsed Power Conference, Digest of Technical Papers 1976-2013, and Abstracts of the 2013 IEEE International Conference on Plasma Science. Held in San Francisco, CA on 16-21 June 2013. U.S. Government or Federal Purpose Rights License

14. ABSTRACT
We are using solid state photoconductive switches to generate wideband microwave pulses with peak powers to 20 MW. A parallel-plate Blumlein transmission line is used to directly feed an exponential taper antenna to produce single pulses with rise times of 200 ps and pulse durations of 340 ps (FWHM). Voltages up to 21 kV have been generated in a I em tall, 12 em wide parallel-plate line. With the switches operated in linear mode, we have demonstrated phasing of several switches to generate a coherent wave. Generated and radiated signals agree very well with numerical calculations. Radiation efficiencies approach 30%. The Blumlein dielectric can be changed to produce a damped waveform, thereby modifying the bandwidth of the signal. We have generated damped waveforms of up to 3 cycles using this method. The parallel-plate geometry lends itself to coupling to an antenna structure to radiate efficiently. The geometry also lends itself to expanding the generator in height and width. We have stacked two generators to nearly double the output power without degrading the pulse characteristics.

15. SUBJECT TERMS

16. SECURITY CLASSIFICATION OF:			17. LIMITATION OF ABSTRACT	18. NUMBER OF PAGES	19a. NAME OF RESPONSIBLE PERSON
a. REPORT	b. ABSTRACT	c. THIS PAGE			
unclassified	**unclassified**	**unclassified**	**SAR**	**4**	

amplitude to the charge voltage and of duration equal to the two-way transit time of the line. If the output impedance of the Blumlein is lower than the load impedance, a damped train of pulses will be delivered to the load with the following parameters: the first pulse will be of amplitude larger than the charge voltage; the duration of each pulse will be equal to the electrical two-way transit time of the Blumlein; the number of pulses and the relative amplitude of each succeeding pulse will be dependent on the ratio of the Blumlein and load impedances. It can be seen from Fig. 1 that the MBA is a classical folded Blumlein line with the impedance of the generator determined by the dielectric constant of the insulator. The impedance was varied from 17.8 W (erected) down to 3 W (erected). The impedance of the output section is constant at about 30 W. The dimensions of the generator section are 11 cm wide, 0.4-2.7 cm long (in the direction of propagation), and 1 cm high (in the field direction). The electrical length of the generator was held constant at 350 ps. The generator uses air or SF_6 for insulation.

The fully developed microwave generator consists of the generator modules shown in Figs. 1 & 2 combined vertically and horizontally to make a powerful, efficient large aperture generator/antenna system. The large radiating area of the generator performs as an aperture with an incident plane wave. The dimensions of the generator aperture are large compared to the wavelengths of interest. The aperture concept mitigates the need for complicated antenna structures while increasing the total power radiated from the generator.

The antenna used for the experiments with the single-module generator depicted in Fig. 2 is an exponentially tapered horn that transitions smoothly from the 1 cm height of the generator to about 40 cm height. The width of the antenna is constant at 11 cm (the width of the generator). The radiation efficiency of the antenna was calculated at 30%[2]. The reflected wave seen in the generator is consistent with this calculation. A detailed antenna pattern was not measured experimentally.

THE PHOTOCONDUCTIVE SWITCHES

The photoconductive switches used to switch the MBA were typically LEC grown Gallium Arsenide (GaAs) fabricated as rectangular tiles 3.5 cm wide by 5 mm tall by 2 mm thick. The switches are installed in the generator as shown in Fig. 1. Contacts are a standard Au:Ge:Ni:Au layered alloy. Note that the switches will short the lower half of the Blumlein uniformly along its length. The laser used to control the switches was a Quantel YG-501 mode locked Nd:YAG laser operating at 1.064 mm producing 50 mJ/pulse at nominally 100 ps duration. This laser produced extrinsic absorption in the GaAs with the number of carriers generated limited by the trap density. The laser was normally used to turn the switches fully on in photoconductive mode with a laser energy of slightly over 1 mJ/cm^2 incident on the switches. For most tests the laser was expanded onto the switches with a set of cylindrical lenses to ensure uniformity and appropriate timing throughout the illuminated area of the switches. The generator was pulse charged with a flat-top pulse of 500 ns duration to prevent switch thermal runaway at the high fields sustained on the switches.

DIAGNOSTICS

In-situ LLNL fabricated capacitive dividers and B-dot probes were the primary diagnostics used to monitor the pulses in the generator and transition section. The signals from these sensors were transmitted through Andrew RF19 cable to Tektronix 7250 transient digitizers. The overall bandwidth of the diagnostic system was approximately 2 GHz, giving a rise time of 175 ps. The radiated waves were measured with an EG&G MGL-8 B-dot sensor with a calibrated response of greater than 2 GHz. The LLNL fabricated probes were calibrated using a 250 V, 100 ps rise pulse.

GENERATOR AND ANTENNA PERFORMANCE

Initial Experiments

Figure 3 shows a typical generator output pulse for a generator dielectric of 3.7 (Delrin) and a generator impedance of 17.8 W. Rise and fall times are < 200 ps (10-90%) and < 150 ps when corrected for diagnostic system response.

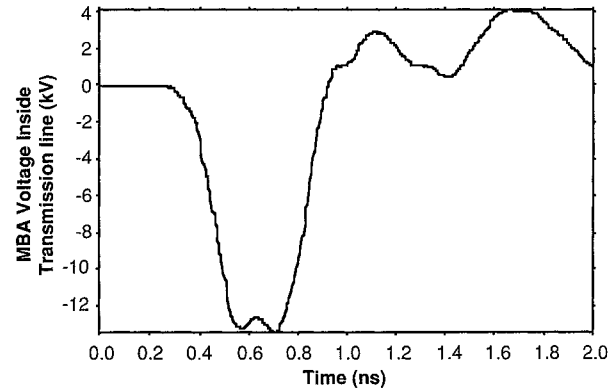

Figure 3. Typical generator output with Delrin dielectric. Note the small second pulse.

The pulse duration is 390 ps FWHM; very close to the design duration. The pulse amplitude in the output line is about 1.2 times the charge voltage; in good agreement with theory. A small second pulse can be seen following the main pulse. This is in reasonable agreement with simulations using a total switch resistance of 0.5 W. This resistance is somewhat higher than expected, probably due to decreased mobility in the GaAs at high fields and carrier generation saturation limited by the density of sites that can be ionized by extrinsic absorption. It should be noted that there was no evidence of unwanted modes seen. The pulse shown in Fig. 3 corresponds to a total generator output power of 4 MW. Voltages of over 25 kV, corresponding to powers of over 19 MW were generated in a single module with similar pulse shapes and characteristic times.

Module Stacking

Since most of the experiments were designed to prove the feasibility of the expandable generator concept, the next experiments were directed to stacking two modules to determine scalability. The output voltage for 2 stacked modules was about 1.8 x that of a single module. The 10% loss was never accounted for but was probably due to a combination of phase errors where the waves combined at the output of the generator and a larger radiating area at the rear of the generator.

Multiple Pulses

Another important experiment performed was the viability of generating a larger number of pulses by changing the dielectric in the Blumlein. Figure 4 shows a typical generator waveform with a generator dielectric constant of 35 (Barium Tetratitanate).

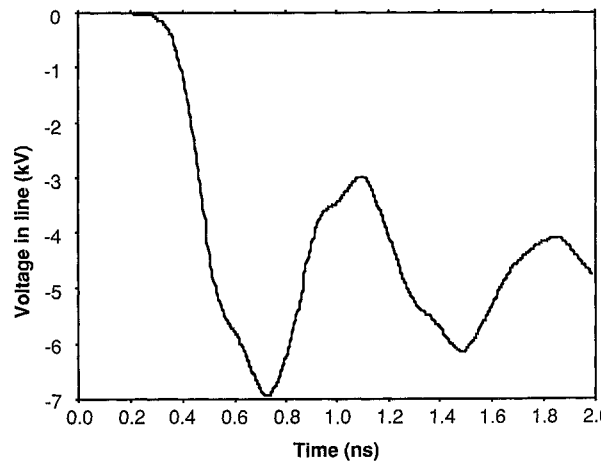

Figure 4. Oscillating waveform produced by a generator with dielectric constant of 35. The peak voltage is about twice the charge voltage.

The fact that the waveform does not return to zero between each pulse can, again, be attributed to the higher-than-expected switch resistance: agreement was good for a simulation performed with 0.25 W

switch resistance. A similar experiment was performed with a generator dielectric constant of 140 (Magnesium Calcium Titanate). Since the line impedance was on the same order as the total switch resistance, results were disappointing, as might be expected. Results to date show that the concept of narrowing the bandwidth by changing the dielectric constant in the generator has merit. It is clear, however, that a very high-Q generator will require some additional lowering of total switch resistance.

Radiated Power and Waveshape

The waveform shown in Fig. 5 is typical of those measured in far-field radiating measurements.

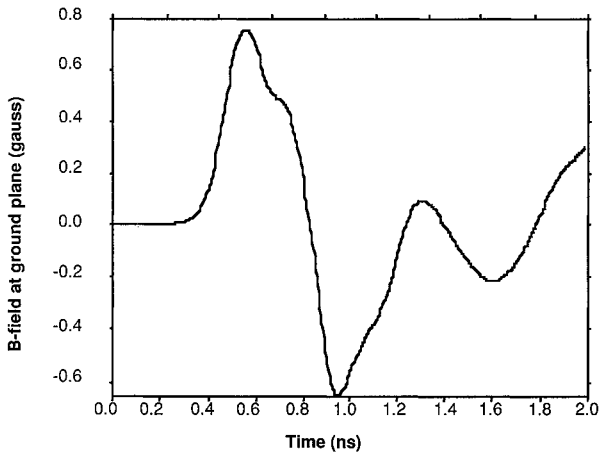

Figure 5. Plot of B-field measured 2 m from the generator.

These measurements were taken on-axis with the generator about 2 m from the antenna aperture. The quantity plotted is the actual B-field measured by the MGL-8 probe. Calculations show that about 1.25 MW was radiated for this shot. If the waveform in Fig. 5 is integrated, the resemblance to the pulse in the line is striking, indicating that the radiated waveform is a close approximation of the derivative of the pulse in the line. An ideal wideband antenna will radiate the derivative of the generated pulse.

SWITCHING EXPERIMENTS

During the course of the MBA experiments it became clear that an improved understanding of photoconductive switches would be required to meet the needs of potential users of UWB generator technology. Repetition rate, system efficiency, and device life must all be improved before photoconductive switches can be used routinely to generate UWB HPM. Having proved the concept, our efforts have returned to basic experiments to determine the switching mechanism of GaAs in the so-called lock-on or "avalanche" mode. In this mode, high fields in the GaAs cause carrier multiplication in the switch, reducing the laser requirements and improving system efficiency. A thorough understanding of the switching mechanism will also lead to improvements in device life. To that end, Rex Booth at LLNL designed a switch with embedded contacts to provide uniform field in the switch and reduce the fields at the contacts; enabling us to separate out the bulk and surface effects in the switches. The switch is shown schematically in Fig 6.

This device has been dubbed the "bead" switch at LLNL. The field enhancement in the switch gap is minimal and the surface field is reduced by a factor of two or more from that in the active switch area. These switches to date have been fabricated from Chromium doped GaAs (Cr:GaAs). Devices with 508 mm switch gaps have been biased to 80 kV/cm DC and over 180 kV/cm pulsed (500 ns pulse). All current devices have been fabricated by grinding the cavity for the electrode in the GaAs with a mechanical grinder, possibly causing surface damage to the GaAs. Experiments are underway to chemically etch the GaAs to avoid this possible surface damage. Initially, the surface treatment of these devices was poor. The outside surfaces of the switch are now being polished to allow better control of the illumination in the gap and to allow infrared microscopy for postmortem analysis.

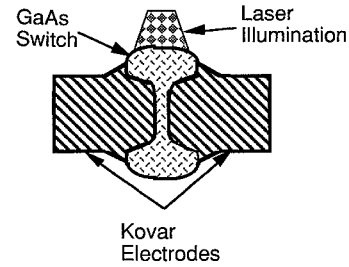

Figure 6. Crossectional diagram of latest switch design showing the embedded electrodes in the GaAs.

The majority of experiments conducted with these switches are designed to improve our understanding of the switching mechanism in "avalanche" switch operation. To that end, an experiment was setup and carefully calibrated to allow monitoring time resolved voltage across the switch and current through the switch simultaneously. The experiment is a 50 W coaxial geometry utilizing a 5 ns charge line, giving a 10 ns pulse duration. Diagnostic response time is about 150 ps. The same Quantel YG-501 laser described earlier was used as the trigger laser. The laser is collimated onto a 1 mm diameter multimode glass fiber: laser energy incident on the switch is typically < 10 mJ. The parameter space of the experiments is specifically designed to allow direct comparison of experimental results with model results: no scaling or conversion of quantities will be required. The active switching region ranges from 0.508 to 0.711 mm gap and approximately 2 mm diameter electrodes. There are plans for larger switch gaps. This gives operating voltages from about 2.5 kV to over 12 kV, depending on the gap, in the avalanche mode. Experiments are being performed to determine "avalanche" delay time, rise time, current through the switch and voltage across the switch as a function of open-state field on the device and laser energy incident on the switch.

Figure 7 is a plot of delay from photoconductive to avalanche rise as a function of open-state switch field for two switches with gaps of 0.508 and 0.711 mm.

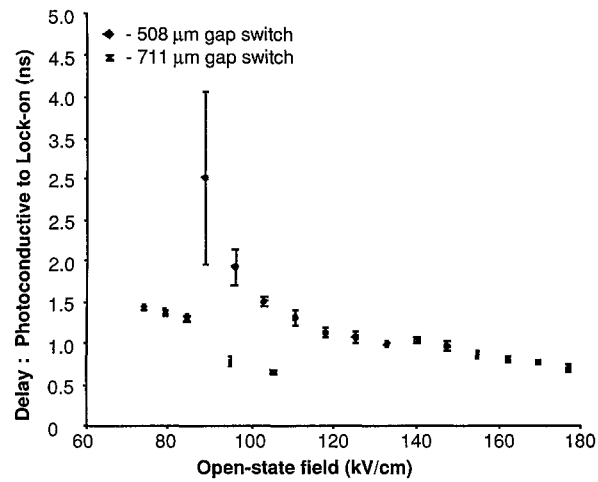

Figure 7. Plot of delay from photoconductive pulse to "avalanche" pulse for 0.508 and 0.711 mm gaps. The error bars are jitter.

Except for the gap, the switches and conditions are identical for both experiments. The laser energy incident on the switch is 2.5 mJ. The error bars represent one s jitter. The lower limit of the data for both switches is the threshold for avalanche operation at this laser energy. The upper limit for the 0.508 mm device is internal self-breakdown. The upper limit for the 0.711 mm device is arbitrary since we wanted to save the switch for other experiments. Note that the delay and jitter are actually smaller for the longer gap at low fields and that the longer gap switch has a lower threshold for avalanche operation. Also note that there seems to be a discontinuity in the data for the longer gap switch at the threshold field for the shorter device. This may indicate that there is a new mechanism occurring at this field and will be investigated further. Using the data in Fig 7 and similar data obtained from Aaron Faulk[3] at Boeing, Yee at LLNL derived values for the avalanche coefficient, a, shown in Fig 8.

Theoretical Ionization Coefficient (a) as function of the electrical field in GaAs deduced from experimental data.

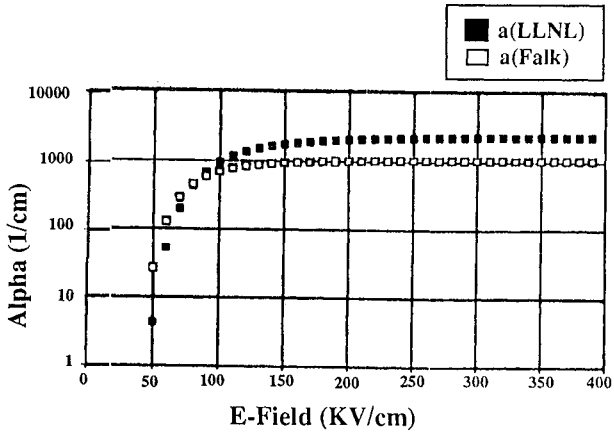

Figure 8. Avalanche coefficient derived from experimental data.

Note that the coefficients for both experiments agree well even though the conditions of the experiments vary widely.

Figure 9 is a plot of current rise for the avalanche pulse as a function of open-state switch field.

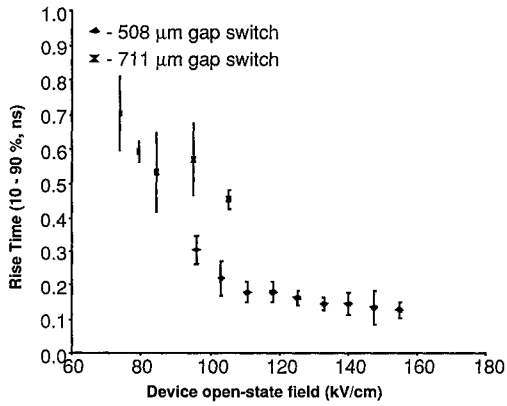

Figure 9. Plot of "avalanche" rise time vs open-state field.

The conditions are the same as for Fig. 8. Note from Fig. 9 that the rise times for the 0.508 mm switch approach 150 ps when corrected for system response. Also note that the rise times for the longer gap switch are longer, which is intuitive in this case. There also seems to be a discontinuity in the rise data for the longer gap switch at the threshold field for the short gap switch. We plan to investigate this discontinuity further.

Figure 10 is a plot of on-state current as a function of open-state field for the same conditions.

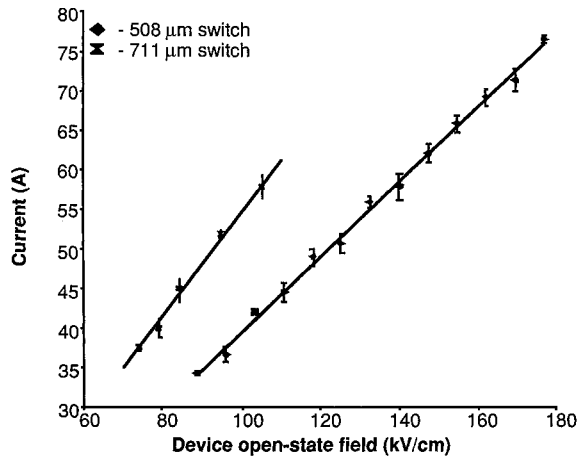

Figure 10. Plot of on-state current vs open-state field. The solid lines are explained in the text.

The line for each set of data represents a least square total error straight line fit to the data. If the fit for each switch is separated into a residual field and residual resistance, the field for both switches is an almost exact match for both devices at 16.57 kV/cm for the 0.508 mm device and 16.60 kV/cm for the 0.711 mm device. The resistance for the 0.508 mm device is 7.8 W and 8.6 W for the 0.711 mm device. These values are confirmed by the direct voltage measurements taken on the devices. The residual field, while higher than those reported elsewhere[4-6], is consistent with the material - Cr:GaAs and the minimal field enhancement present in the switch.

FUTURE PLANS

We do not plan to continue experiments on wideband microwave generation and radiation in the foreseeable future. This work proved the viability of the concept.

Future experiments and modeling should continue to concentrate on formulating a theory for switching mechanisms and improving device life. Special samples of several variations of GaAs material and fabrication technique are being sent to Old Dominion University to have a full characterization of traps and defects performed. These material properties will be used as input to the 1-dimensional drift-diffusion code developed here at LLNL. Output from the code will be compared directly with experimental data.

U.V. microscopy to look into the bulk of the switch will be used to inspect failed switches for signs of internal damage. The switches will be dissected and the pieces tested to determine if a quadrant of the switch failed.

CONCLUSIONS

Photoconductive switches are a prime candidate for UWB microwave generation for many applications. If efficiency and switch device life issues can be addressed successfully, photoconductive switches will be usable for all aspects of UWB HPM, including high power, high rep-rate, compact size, and frequency and bandwidth agility issues.

The prime research areas are efficiency and life time. The efficiency issues will be completely mitigated by the use of avalanche mode: rise times of < 200 ps have been observed. Device life is still a critical problem that must be addressed. Issues of filamentation and postmortem analysis must be pursued. An understanding of the basic physics of the switching mechanism will certainly aid in both efficiency and device life studies.

REFERENCES

1.R. N. Edwards, K. W. Reed, W. C. Nunnally, and C. V. Smith, Jr., "Investigation of Optically Induced Avalanching in GaAs," Proceedings of the 7th IEEE Pulsed Power Conference, June 11-14, 1989, pp 433-436.

2.R. M. Searing, "Focusing E-plane Sectoral Horn at Aperture," Private communication.

3.R. A. Faulk and F. C. Adams, "Temporal Model of Optically Initiated GaAs Avalanche Switches," SPIE OPTCON Proceedings, vol. 1378 November 5 & 6, 1990, pp 70-81.

4.M. D. Pocha and R. L. Druce, "35 kV GaAs Subnanosecond Photoconductive Switches," IEEE Transactions on Electron Devices, vol. TED-37, no. 12, December 1990.

5.F. J. Zutavern, G. M. Loubriel, et al, "Photoconductive Semiconductor Switch Experiments for Pulsed Power Applications," IEEE Transactions on Electron Devices, vol. TED-37, no. 12, December 1990.

6.M. K. Browder and W. C. Nunnally, "Investigation of Optically Induced Avalanching in GaAs," Proceedings of the 7th IEEE Pulsed Power Conference, June 11-14, 1989, pp 433-436.